Atom probe tomography of carbides in Fe-Cr-(W)-C steels

Alexander Gramlich, Maria Auger, André Schneider, Michael Moody*

A. R. M. Gramlich

Institut für Eisenhüttenkunde, RWTH Aachen, Intzestraße 1, 52072 Aachen Germany
E-mail: alexander.gramlich@iehk.rwth-aachen.de

Dr. M. A. Auger
Physics Department, Universidad Carlos III de Madrid. Av Universidad 30, 28911 Leganés, Madrid, Spain

Dr. André Schneider
Vallourec Research Center Germany, 40472 Düsseldorf-Rathingen, Germany

Prof. Michael P. Moody
Department of Materials, University of Oxford, Parks Road, OX1 3PH Oxford, UK

Keywords: Atom probe tomography, carbides, ferritic-martensitic steels, precipitations

In this study, Fe-Cr-C and Fe-Cr-W-C alloys were characterised using atom probe tomography. The alloys have been heat treated at 1070°C for 30 min and subsequently at 780°C for various time periods. Carbide formation was observed at each state. Cr-C precipitates smaller than 5 nm in radius for short heat treatment times and larger than 50 nm for heat-treatment times greater than 1000 s were observed. It was found that the movement of the interfaces decreases for the Fe-Cr-C alloys, if the annealing time is increase and the interface movement in Fe-Cr-W-C alloys is in general faster than in the Fe-Cr-C alloys. Furthermore, kinetic assumptions for the carbide nucleation from previous study have been verified. A decrease of the microhardness with increasing aging time was detected and could be connected to the growth of carbides and the decreasing carbon content soluted in the matrix. The aim of this study is to measure the change in chemical compositions across phase interfaces between matrix and precipitates to obtain a better understanding of the precipitation process.

1. Introduction

Ferritic-martensitic Cr-steels have drawn significant attention during the recent decades.[1-4] Several international projects were initiated to design advanced steel alloys with good creep and oxidation resistance for high temperature applications in so called Ultra Super Critical (USC) Power Plants.[5-7] One of these studies targeted the development of a heat resistant 12 wt.% Cr ferritic steel for usage at 650°C.[5] The alloy design was supported by several thermodynamic calculations and computer-simulations on diffusion controlled phase transformations.[7]

For the given alloys and heat treatments of interest it was reported that different types of carbides, M_3C_6, $M7C_3$ and $M_{23}C_6$ are expected to occur in the matrix; it was also predicted that only $M_{23}C_6$ would be left in the matrix in the equilibrium state, as it is the only thermodynamically stable precipitate.[7] Bjärbo et al. showed that unstable carbides dissolve after their metastable precipitation and Park et al. revealed a transformation of M_7C_3 into $M_{23}C_6$.[8,9] In W containing Fe-Cr alloys, $M_{23}C_6$ is further stabilised by the presence of W.[10] The aim of this study is to provide further atomic-scale insights into the precipitation behaviour of Fe-Cr-(W)-C model alloys by investigating and comparing the chemical compositions across phase interfaces between matrix and carbides for Fe-12Cr-0.1C and Fe-12Cr-3W-0.15C (wt. %) alloys after different heat-treatments using atom probe tomography (APT); optical and electron microscopy imaging together with microhardness measurements were also used to complete this study. Therefore, these work intents to verify the reliability of models for USC Power Plants.

2. Experimental Procedure

Two different 0.5 kg laboratory batches with nominal compositions Fe-12Cr-0.1C (wt. %) and Fe-12Cr-3W-0.15C (wt. %) were melted in a vacuum induction furnace. The bulk composition is presented in **Table 1** together with the nomenclature that will be used. Both alloys were submitted to austenitisation in air at 1070°C for 30 minutes. Samples of the Fe-12Cr-0.1C (wt. %) alloy were then aged at 780°C for 100 s, 1000 s and 10000 s, and

quenched in water. The Fe-12Cr-3W-0.15C (wt. %) alloy was aged at 780°C for 10000 s and quenched in water. Microstructure observation was made by optical microscopy (OM) and scanning electron microscopy (SEM) using a Leica DM microscope and a Zeiss Sigma Field Emission Gun-SEM. The samples were prepared by grinding, polishing and etching in a V2a etching-solution. Hardness measurements were made by using a universal Vickers indenter. Three indentations were made per sample using a load of ~ 10 N and a dwell time of 15 s. Specimens suitable for APT analysis were prepared by cutting the bulk sample into matchsticks (1 mm x 1 mm x 20 mm) that were ground and polished with SiC paper before being submitted to a standard 2-stage electro-polishing.[11] Additionally, some samples were prepared by the standard FIB lift-out method,[12] using a Zeiss Auriga FIB/SEM instrument. APT was carried out on a CAMECA LEAP 3000X HR™ and on a CAMECA LEAP 5000X HR™, using voltage or laser mode. The experiments were carried out at a temperature of 50K. In voltage mode a repetition rate of 200 kHz and 20% pulse fraction was used. In laser mode a repetition rate of 200 kHz and laser energies of 0.40 nJ (LEAP 3000) and 0.040 nJ (LEAP 5000) were used. CAMECA IVAS™ commercial software was used for data analysis and reconstruction.

DICTRA software was used to simulate the transformation kinetics in the Fe-12Cr-3W-0.15C (wt. %) alloy aged for 10000 s.[13]

3. Results

The microstructure of the different sample group is shown in **Figure 1** (OM) and **Figure 2** (SEM). Small carbides with an approximated size of < 200 nm are homogeneously distributed in the matrix after 100 s of aging. With increasing aging time a coarsening of the carbides takes place, which results in an inhomogeneous carbon distribution. Additionally, the micro-hardness of the different samples was tested. The results can be seen in **Figure 3**.

For each group, carbides could be detected inside the Atom Probe samples. For the analyses, it is necessary to choose a precipitation boundary value with a significant difference between

the matrix and the carbide composition in order to get a smooth interface. A 35 at. % has been chosen in this case, as this value also seems to be around the inflexion point of the chromium-content-curves. **Figure 4** displays 3D ion map reconstructions of representative volumes from each sample. Carbon enriched regions and, therefore, potential carbides, can be observed in all of them.

Many small precipitates can be observed in the 100s sample (Figure 4a). **Figure 5**a presents analysis of their size distribution in terms of the precipitate radius, which ranges from 1 to 4.2 nm with an average value of 2.78 ± 1.13 nm. The radius was calculated from the volume inside the iso-surfaces, estimating a near sphere-shape morphology. In all the other samples the precipitates are much larger than these (> 50 nm), hence only a fraction of each carbide could be captured and analysed. $M_{23}C_6$ carbides in these alloys are expected to have a mean diameter of around 100 nm,[10] which makes difficult to observe them completely within the nanometric volumes in the field-of-view of APT experiments. In the 1000s and the 10000s samples (Figure 4b and 4c), carbides were observed to be adjacent to regions with a higher apparent atomic density in the APT reconstructions. These high density regions are indicative of the presence of interfaces. It is well established that interfaces, such as grain boundaries, can result in trajectory aberrations in the APT experiment, resulting in these features as being represented by a region of aberrantly high density in the data. This can enable the presence of such features to be identified via APT, particularly in those cases where no significant solute segregation is observed.

To analyse the precipitates, an interface Cr concentration value was chosen to define smooth isosurfaces enclosing precipitates.

The proximity histogram analysis in Fig. 5c compares the Fe, Cr and C distribution in the 10000s and 10000s_W samples. The Fe, Cr and C content in the matrix are similar across both alloys. However, the Fe and Cr contents in the precipitate in 10000s_W are slightly lower and C content slightly higher than in 10000s.

Fig. 5d presents the chemical composition across the phase interface for the 10000s_W sample in comparison with a DICTRA simulation of carbide growth in this alloy.

The Fe, Cr, C and W contents in the matrix and in the precipitates are calculated from the proximity histograms shown in Fig. 5b; they are summarized in **Figure 6**a and 6b, respectively.

4. Discussion

The LOM and SEM images reveal that an overall coarsing of the carbides takes place as expected when the aging time increases. In the beginning, the carbon is nearly completely homogenously distributed. This change in carbon distribution explains the decrease of the microhardness with longer annealing times. As more and larger carbides are formed after longer annealing times, less carbon is available for solute solution hardening. The SEM mircrographs are showing small regions which might be enriched with chromium, which fits to the measured particles with APT. Therefore, it can be concluded, that the measured particles with APT might be seen as representative, as the morphology supports the observations with OM and SEM. After a heat treatment of 100 s, C rich precipitates were already observed. Due to the very early state of carbide formation and the very small size of the precipitates (2.78 ± 1.13 nm) it is not possible to confirm the carbide type. This measured size value agrees with dimensions chosen by Schneider and Inden to simulate the kinetics of precipitation reactions in ferritic steels.[7] According to these simulations, after 10000s only the $M_{23}C_6$ carbide type is present, since the other metastable carbides were already dissolved. The measured C content inside the precipitates was lower than the expected ~20.7 at. % for $M_{23}C_6$ (Fig. 6b). However, such discrepancies have previously been well described in the literature, with a systematic underestimation of C content in carbides due to the combination of several effects during the evaporation and detection in APT experiments.[14-16] This represents the difference between the detected and the expected carbon content in the carbides.

It is apparent from Fig. 6b that the Cr and C content inside the precipitates increases with the heat treatment time. The Cr content in the matrix (Fig. 6a) decreases with the heat treatment time, while the C content in the matrix remains at a low level. But especially for the sample aged for 100 s the chemistry determined by APT has to be questioned. The volume of the precipitates is small compared to the other heat treatments, which leads to a lower statistic quality of the determined chemistry due to a large effect of trajectory aberrations on small precipitates. [11]

The matrix/carbide interface width, which can be measured via the proximity histograms in Figs. 4b and 4c, can be linked to the speed of its movement. The measured interface width in 100s and 1000s had a similar value of ~ 4.0 nm, so the interface movement would be similar in that time range. An interface size of 4.6 nm was measured in 10000s, 15% larger than in 1000s, suggesting a slower interface movement at the longer aging time. Notably, for the 10000s_W the matrix/carbide interface size was 2.6 nm, 44% smaller than in 10000s, suggesting a faster movement of the phase interface in this case. These results are in agreement with the simulations.[7]

For the quaternary Fe-Cr-W-C alloy, the concentration results appear to agree with the DICTRA simulation (Fig. 5d). Although there is some difference between the measured and calculated contents for Fe, C and, particularly, Cr, the W concentration around the phase interface fits, implying that the assumed conditions specified in Ref 7 for the kinetic simulations seem to be valid.

Concerning the nucleation and growth of chromium carbides it has be shown, which carbide compositions can be found for different states of nucleation. However, the results are not representative in cases of nucleation density or nuclei size. This has to investigated in a different study, using correlative transmission electron microscopy (TEM) or high resolution transmission electron microscopy (HRTEM).

5. Conclusions

The present study adds insights to the complex topic of carbide precipitation and growth in ferritic-martensitic Cr-steels.:

- Cr and C enriched regions can be found in the matrix even after very short heat-treatment times, which are the precursors for the carbide growth. Precipitates smaller than 5 nm (radius = 2.78 ± 1.13 nm) in size form at short times, being at least one order of magnitude larger at longer aging times up to 10000 s.
- The phase interface seems to move at a similar speed up to 1000 s of aging time and slower at 10000 s in Fe-12Cr-0.1C (wt. %) alloys. A faster interface movement is observed in Fe-12Cr-3W-0.15C (wt. %).
- For the quaternary alloy, a validation of assumed kinetic conditions was achieved.
- The drop in hardness after 10000s, both in the Fe-12Cr-0.1C (wt. %) and Fe-12Cr-3W-0.15C (wt. %) samples indicates the change in carbon distribution and chromium carbide coarsing over time.

Acknowledgements

Funding from UK EPSRC Project grants EP/M022803/1 and EP/P001645/1 are gratefully acknowledged. The present work was done during an academic visit of A. Gramlich in the Department of Materials of University of Oxford.

Received: ((will be filled in by the editorial staff))
Revised: ((will be filled in by the editorial staff))
Published online: ((will be filled in by the editorial staff))

References

[1] M. Hayakawa, K. Yamaguchi, M. Kimura, K. Kobayashi, *Mater Lett* **2004**, 58, pages 2565-2568

[2] H. Ghassemi-Armaki, R.P. Chen, K. Maruyama, M. Yoshizawa, M. Igarashi, *Mater Lett* **2009**, 63, pages 2423-2425

[3] I.M. Moustafa, M.A. Moustafa, A.A. Nofal, *Mater Lett* **2000**, 42, pages 371-379

[4] J.W. Schinkel, P.L.F. Rademakers, B.R. Drenth, C.P. Scheepens, *Journal of Heat Treating* **1984**, 3, pages 237–248

[5] V. Knezevic, G. Sauthoff, J. Vilk, G. Inden, A. Schneider, R. Agamennone, W. Blum, Y. Wang, A. Scholz, C. Berger, J. Ehlers, L. Singheiser, *Isij Int* **2002**, 42, pages 1505-1514

[6] V. Knezevic, J. Balun, G. Sauthoff, G. Inden, A. Schneider, *Mat Sci Eng a-Struct* **2008**, 477, pages 334-343

[7] A. Schneider, G. Inden, Simulation of the kinetics of precipitation reactions in ferritic steels, *Acta Mater* **2005**, 53, 519-531

[8] A. Bjärbo, M. Hättestrand, *Metall Mater Trans A* **2001**, 32, pages 19–27

[9] I.M. Park, T. Fujita, K. Asakura, *T Iron Steel I Jpn* 20 **1980**, 20, pages 99-107

[10] A. Bjarbo, Scand J Metall **1994**, 23, pages 103-112

[11] B. Gault, Atom probe microscopy, Springer, New York, 2012.

[12] K. Thompson, D. Lawrence, D.J. Larson, J.D. Olson, T.F. Kelly, B. Gorman, *Ultramicroscopy* **2007**, 107, pages 131-139

[13] A. Borgenstam, A. Engstrom, L. Hoglund, J. Agren, *J Phase Equilib* **2000**, 21, pages 269-280

[14] M. Thuvander, J. Weidow, J. Angseryd, L.K.L. Falk, F. Liu, M. Sonestedt, K. Stiller, H.O. Andren, *Ultramicroscopy* **2011**, 111, pages 604-608

[15] R.K.W. Marceau, P. Choi, D. Raabe, *Ultramicroscopy* **2013**, 132, pages 239-247

[16] H.S. Kitaguchi, S. Lozano-Perez, M.P. Moody, *Ultramicroscopy* **2014**, 147, pages 51-60

Tables:

Table 1. Chemical composition of the alloys.

Alloy)	Fe (wt. %)	Cr (wt. %)	C (wt. %)	W (wt. %)	Aging time	Nomenclature
					100 s	100s
Fe-12Cr-0.1C	Bal.	11.62	0.18	0	1000 s	1000s
					10000 s	10000s
Fe-12Cr-3W-0.15C	Bal.	11.71	0.143	2.671	10000 s	10000s_W

Figures:

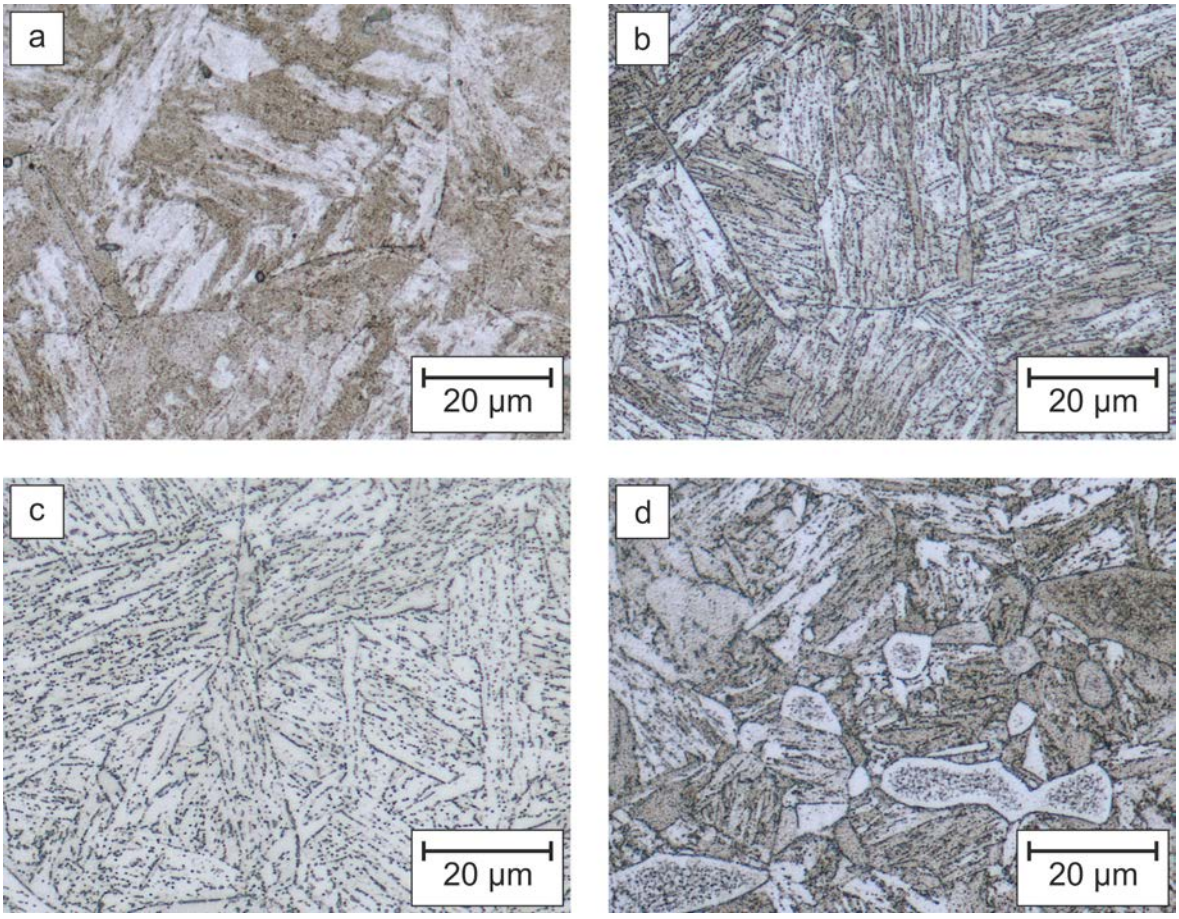

Figure 1. Optical micrographs of the investigated samples; (a) 100s, (b) 1000s, (c) 10000s, (d) 10000s_W.

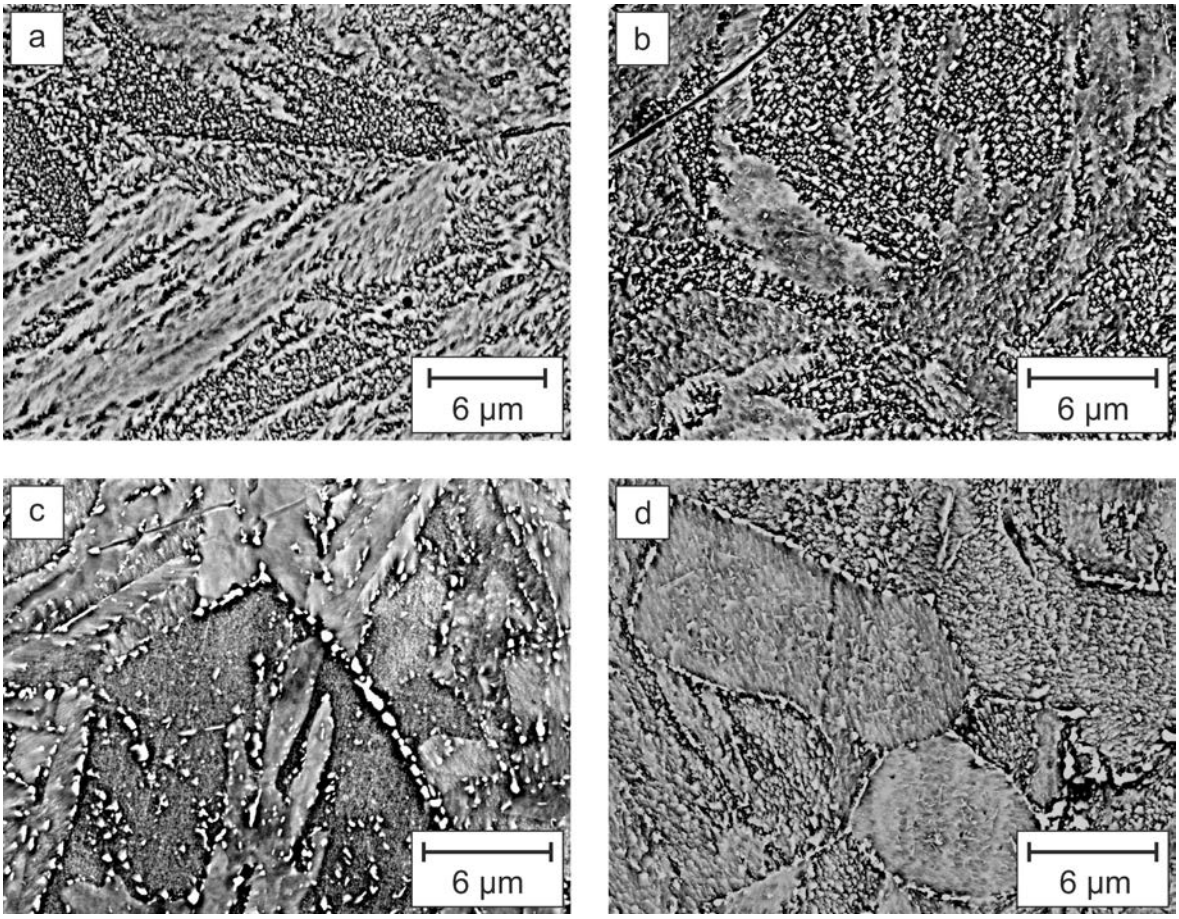

Figure 2. BSE-SEM images of the investigated samples; (a) 100s, (b) 1000s, (c) 10000s, (d) 10000s_W.

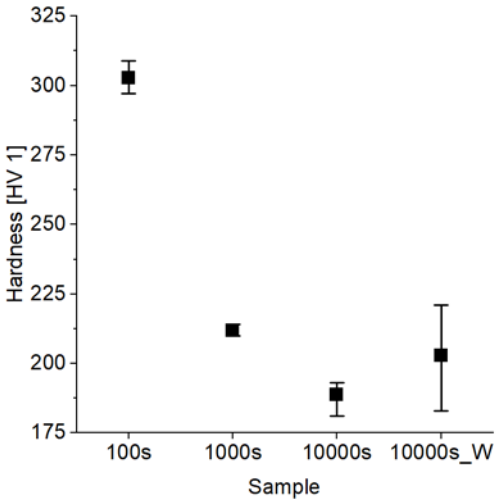

Figure 3. Micro-hardness of the different sample groups.

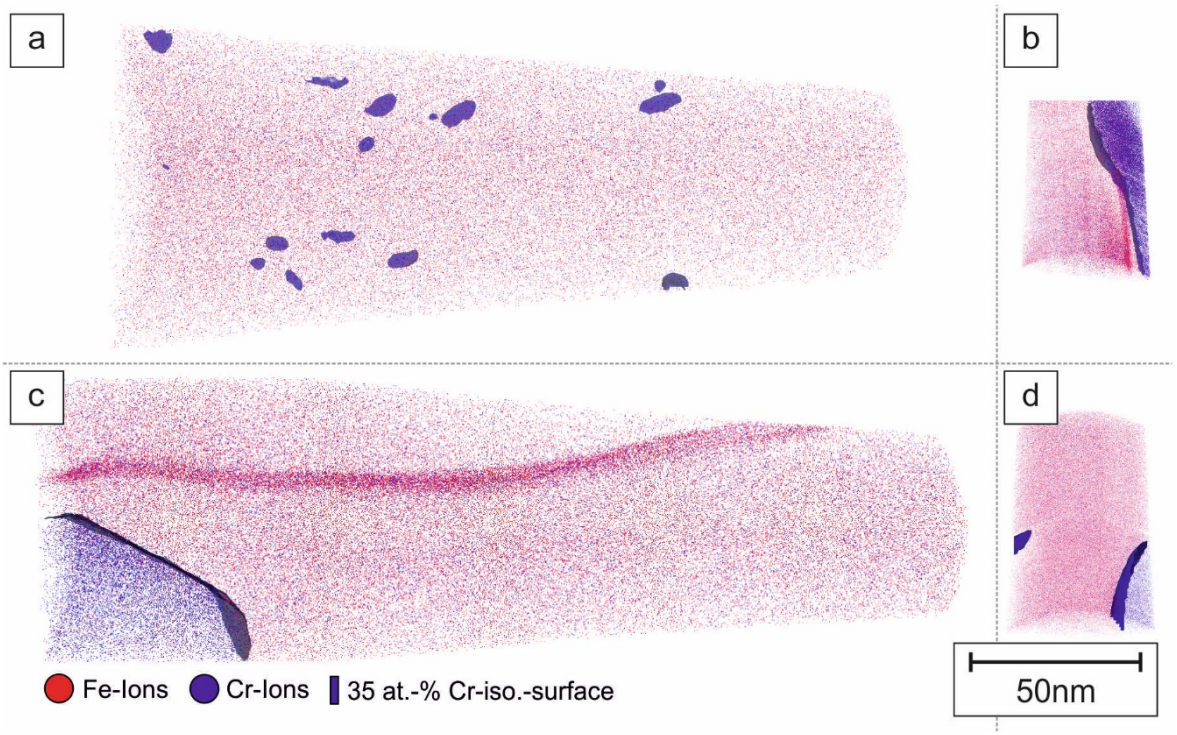

Figure 4. APT-3D reconstructions for (a) 100s, (b) 1000s, (c) 10000s, and (d) 10000s_W

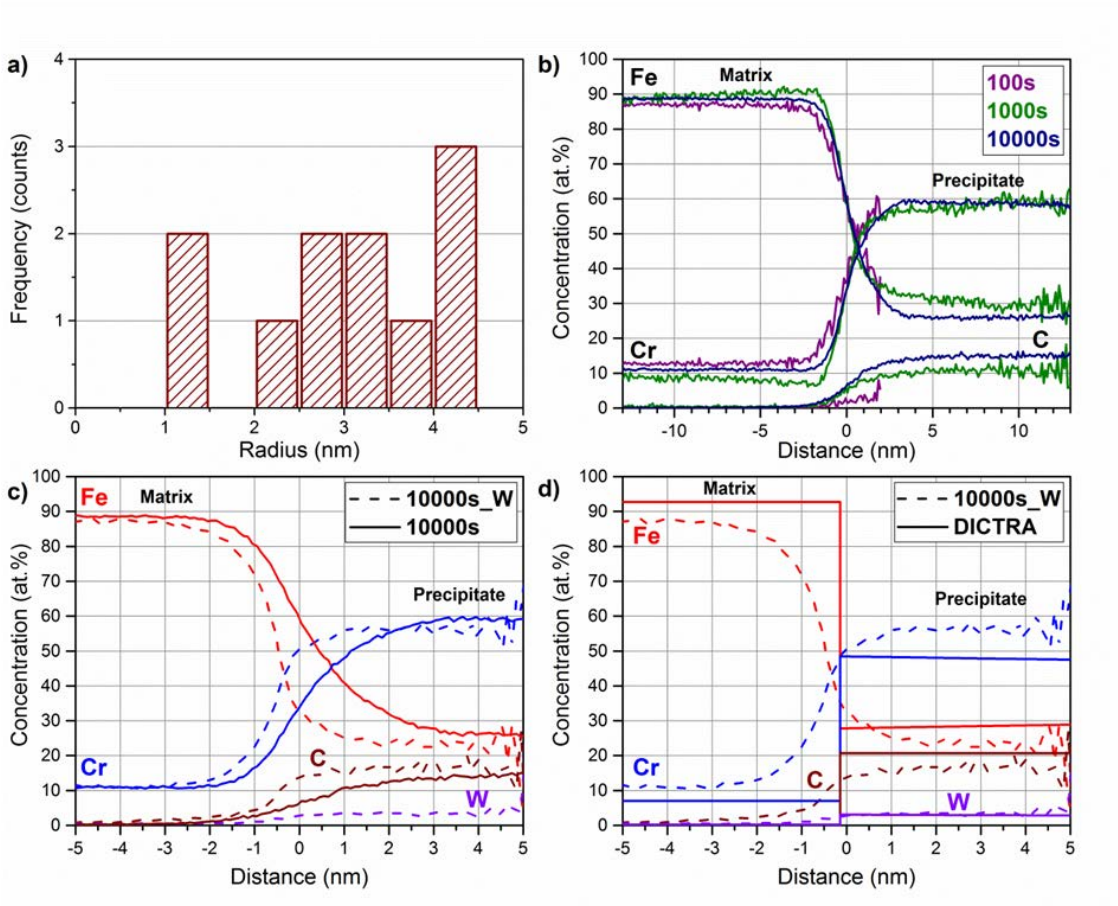

Figure 5. (a) Distribution of precipitate size in 100s. (b) Proximity histograms for 100s, 1000s and 10000s. (c) Proximity histograms of 10000s and 10000s_W. (d) Proximity histogram and DICTRA simulations for 10000s_W.

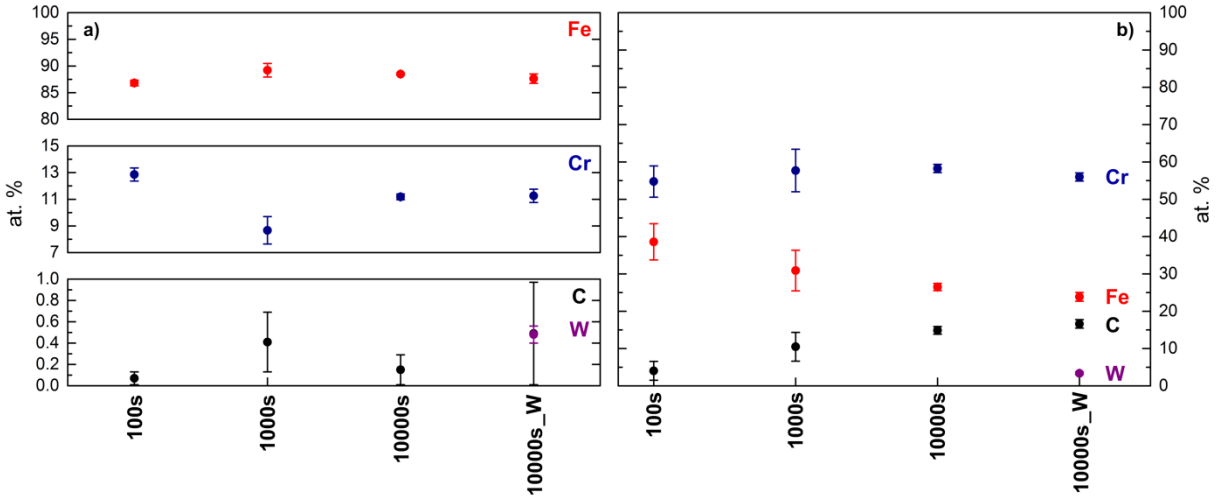

Figure 6. Fe, Cr, C and W (at. %) contents (a) in the matrix and (b) in the precipitates of all the samples.

Ferritic-martensitic steels are often used for applications in power plants. These steels are chromium alloyed to improve the mechanical properties and corrosion resistance. Due to the high amounts of chromium, several different chromium carbides can form and grow in this steels. In this study, different aging states of carbides are investigated using atom probe tomography.

Chromium Carbide Analyses

Alexander Gramlich*, Maria Auger, André Schneider, Michael Moody

Atom probe tomography of carbides in Fe-Cr-(W)-C steels